

# APOE $\epsilon$ 4-Associated Hippocampal Atrophy Trajectories Across the Alzheimer's Disease Continuum: A Systematic Review, Meta-Analysis, and Longitudinal Validation

Minnuo Cai<sup>1,3</sup>, Hang Lei<sup>1</sup>, Yuetong Zhang<sup>1</sup>, Jiaxiang Zou<sup>1</sup>, Wanjing Cao<sup>1</sup>, Yiquan Wang<sup>1,2,3,\*</sup>, Kai Wei<sup>1,\*</sup>,  
for the Alzheimer's Disease Neuroimaging Initiative<sup>†</sup>

<sup>1</sup> Xinjiang Key Laboratory of Biological Resources and Genetic Engineering, College of Life Science and Technology, Xinjiang University, Urumqi, Xinjiang, China

<sup>2</sup>College of Mathematics and System Science, Xinjiang University, Urumqi, Xinjiang, China

<sup>3</sup>Shenzhen X-Institute, Shenzhen, China

\*Corresponding authors: ethan@stu.xju.edu.cn, kaiwei@xju.edu.cn

## Abstract

**Background:** The role of APOE- $\epsilon$ 4 in hippocampal atrophy is contested. We aimed to determine whether it functions as a static risk factor or an amyloid- $\beta$  ( $A\beta$ )-dependent modulator of neurodegeneration.

**Methods:** We integrated a systematic meta-analysis of 18 studies ( $N = 3,781$ ) with longitudinal validation using linear mixed-effects models in the NACC and ADNI cohorts ( $N > 5,000$ ), employing biomarker stratification to test for gene-pathology interactions.

**Results:** The meta-analysis confirmed significant atrophy in APOE- $\epsilon$ 4 carriers but with high heterogeneity. Longitudinal analysis resolved this by identifying a crucial interaction: in  $A\beta$ -negative individuals, carrier atrophy rates were indistinguishable from non-carriers. However,  $A\beta$  positivity triggered a dramatic, dose-dependent acceleration in atrophy among carriers, with homozygotes declining over three times faster.

**Conclusions:** APOE- $\epsilon$ 4 acts as a potent, conditional accelerator of neurodegeneration, not an independent driver. Its deleterious effect is contingent on the presence of  $A\beta$  pathology. Clinical risk stratification should therefore integrate amyloid status with APOE genotype to accurately predict structural progression.

**Keywords:** AD Spectrum, APOE- $\epsilon$ 4, Hippocampal Volume, Systematic Review, Amyloid Interaction

## 1 Introduction

Alzheimer's Disease (AD) is biologically defined by the accumulation of amyloid- $\beta$  ( $A\beta$ ) and tau proteins, and characterized by progressive hippocampal atrophy as a key marker of neurodegeneration [1–3]. While the  $\epsilon$ 4 allele of Apolipoprotein E (APOE- $\epsilon$ 4) is recognized as the strongest genetic risk factor for late-onset AD [4,5], the precise nature of its impact on hippocampal integrity remains incompletely understood.

Specifically, critical knowledge gaps persist regarding the timing, mechanism, and dosage of APOE- $\epsilon$ 4-related atrophy. First, conflicting evidence exists regarding the temporal origin of structural loss: the developmental hypothesis suggests

a static, congenital phenotype [6, 7], whereas the neurodegenerative hypothesis proposes an accelerated decline in later life [8–10]. Second, the allele dosage effect, specifically whether homozygous ( $\epsilon$ 4/ $\epsilon$ 4) carriers exhibit disproportionately severe atrophy compared to heterozygotes, is not fully characterized, leaving the linearity of potential genetic toxicity uncertain [11, 12]. Third, a qualitative divergence exists regarding whether APOE acts through direct structural toxicity [13] or primarily as an upstream modulator dependent on amyloidosis [9].

These unresolved discrepancies likely stem from both biological and methodological limitations in prior literature. Biologically, traditional volumetric analyses often overlook occult pathologies, such as asymptomatic amyloidosis, in clinically normal populations [14, 15]. This may confound independent genetic effects with early-stage disease processes. Methodologically, previous studies have been constrained by modest sample sizes, varying measurement protocols, and demographic heterogeneity [16]. This variability limits statisti-

<sup>†</sup> Data used in preparation of this article were obtained from the Alzheimer's Disease Neuroimaging Initiative (ADNI) database ([adni.loni.usc.edu](http://adni.loni.usc.edu)). As such, the investigators within the ADNI contributed to the design and implementation of ADNI and/or provided data but did not participate in the analysis or writing of this report. A complete listing of ADNI investigators can be found at: [http://adni.loni.usc.edu/wp-content/uploads/how\\_to\\_apply/ADNI\\_Acknowledgement\\_List.pdf](http://adni.loni.usc.edu/wp-content/uploads/how_to_apply/ADNI_Acknowledgement_List.pdf)

cal power and hinders a robust, consensus-based assessment of the APOE effect size across the AD continuum.

To address these gaps, this study employs a comprehensive, hierarchical design moving from macro-level synthesis to mechanistic analysis. We first conduct a systematic meta-analysis to integrate large-scale data, overcoming individual study heterogeneity to quantify the aggregate effect of APOE- $\varepsilon$ 4. Subsequently, we utilize dual-cohort longitudinal validation (NACC and ADNI) with biomarker stratification [17, 18]. This integrated approach aims to elucidate whether APOE- $\varepsilon$ 4-related atrophy represents a dose-dependent, intrinsic feature or a conditional phenomenon associated with the synergistic interaction of amyloid pathology [9].

## 2 Methods

### 2.1 Meta-analysis Strategy

This systematic review and meta-analysis was conducted and reported in accordance with the PRISMA guidelines [19] (Figure 1). We performed a systematic search of PubMed, Embase, the Web of Science Core Collection, and the Cochrane Library for original research published up to August 2025, following the Population, Intervention, Comparison, and Outcome (PICO) framework. The entire screening process was managed using the Covidence online platform.

A notable challenge in this field is the use of overlapping data from large, shared databases across multiple publications. To address this, we implemented a specific protocol: if multiple studies originated from the same primary data source, we included only the publication that was most recent or provided the largest and most comprehensive sample. This step was essential to ensure the independence of the included cohorts and refined our initial selection from 24 eligible articles ( $N = 7326$ ) to a final set of 18 unique studies ( $N = 3781$ ) [6, 20–42]. For the quantitative synthesis, we extracted sample sizes, means, and standard deviations of hippocampal volume for both APOE- $\varepsilon$ 4 carriers and non-carriers from these publications.

The effect size was calculated as the Standardized Mean Difference (SMD) using Hedges' g. A random-effects model, with the between-study variance estimated using Restricted Maximum-Likelihood (REML), was employed to pool effect sizes [43]. The Hartung-Knapp adjustment was applied for more robust confidence intervals. Heterogeneity was quantified using the  $I^2$  statistic [44]. To investigate sources of heterogeneity, we first performed subgroup analyses based on clinical diagnosis, APOE genotype dosage, and ICV correction methods [45]. Second, we conducted univariable random-effects meta-regressions to assess the potential moderating effects of mean participant age and sex distribution (Figure 2).

To evaluate the stability and robustness of our results, several additional analyses were conducted. We performed a leave-one-out sensitivity analysis to assess the influence of each individual study on the overall pooled estimate. Bau-

jat plots were generated to visually identify studies contributing most to both overall heterogeneity and the pooled effect. Furthermore, we implemented a multiverse analysis to test whether the main conclusion was robust to different analytical choices regarding the removal of potential outliers. Finally, publication bias was assessed using Egger's regression test, and the trim-and-fill method was used to estimate a bias-corrected effect size [46]. All statistical analyses were performed in R (version 4.5.2).

### 2.2 Longitudinal Cohorts and Participants

We utilized longitudinal data from two independent multicenter cohorts: the National Alzheimer's Coordinating Center (NACC) and the Alzheimer's Disease Neuroimaging Initiative (ADNI).

The NACC Uniform Data Set was utilized to assess the gene-dose effect in a large-scale clinical population [18, 47]. Using the dataset from the September 2025 data freeze (covering visits between September 2005 and September 2025), we identified 3,986 participants who had available pre-processed longitudinal hippocampal volume measurements and confirmed APOE genotyping.

The ADNI dataset was employed to investigate the interaction between genetics and pathology [48, 49]. From the data downloaded in August 2025, we selected a subset of 1,947 participants based on the concurrent availability of longitudinal hippocampal volume measurements, confirmed APOE genotyping, and baseline Cerebrospinal Fluid (CSF) biomarker levels (A $\beta$ 42, p-Tau181, and t-Tau). No raw MRI images were processed in this study; all volumetric data were obtained directly from the study repositories.

To ensure the independence of the discovery and validation cohorts, systematic cross-verification was performed to confirm that there were no overlapping subjects between the two datasets based on unique identifiers and demographic profiles.

### 2.3 Data Preprocessing and Quality Control

For the NACC dataset, a dedicated preprocessing and quality control (QC) pipeline was applied. First, to prevent endogeneity issues arising from disease progression itself, each subject's clinical diagnosis was locked to their baseline status. Second, a two-stage QC was performed: for cross-sectional QC, we fitted a linear model of hippocampal volume adjusted for age, sex, eTIV, and baseline diagnosis, and observations with standardized residuals exceeding a conservative threshold of  $\pm 4$  SD were excluded. For longitudinal QC, we calculated the annualized rate of volume change and removed trajectories with biologically implausible changes, such as an annual volume increase greater than 20% or a loss exceeding 30%. Finally, to optimize model performance and interpretability, the age covariate was centered and eTIV was scaled.

To construct a robust dataset for longitudinal analysis, a systematic preprocessing and quality control (QC) pipeline was applied to the ADNI data. To mitigate potential confounding from disease progression, each subject's clinical di-

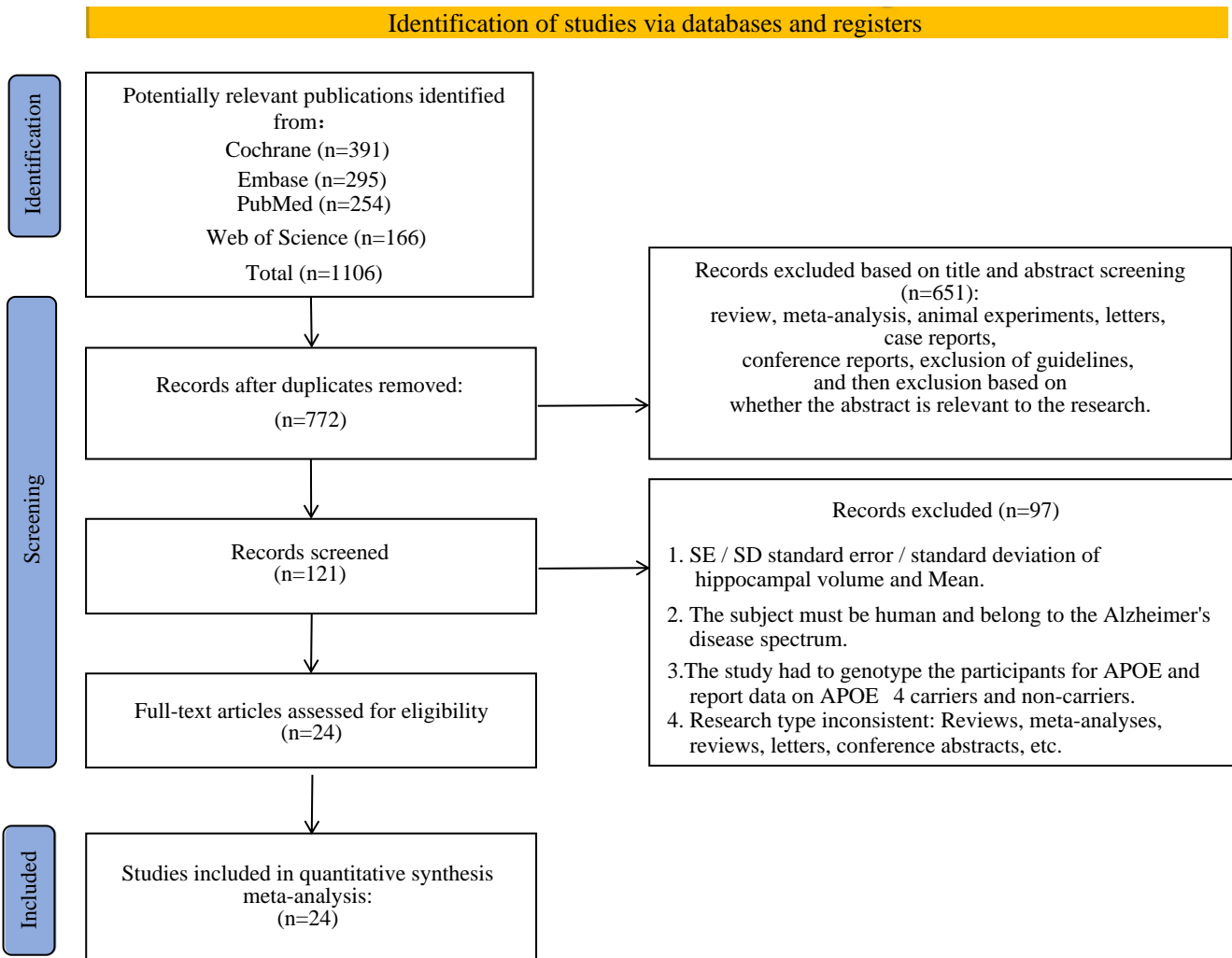


**Figure 1:** PRISMA flow diagram of the study selection process. The flowchart depicts the stepwise exclusion of records from identification to final inclusion. A total of 1,106 records were initially identified from four databases (Cochrane, Embase, PubMed, and Web of Science). Following duplicate removal, 772 records underwent title and abstract screening. Subsequently, 121 full-text articles were assessed for eligibility, with 97 excluded for not meeting the predefined inclusion criteria (see Supporting Information for details). Ultimately, 24 studies met all inclusion criteria for the quantitative meta-analysis.

agnosis was fixed to their baseline status. The analysis was restricted to participants with at least two valid neuroimaging follow-up visits, ensuring the reliability of individual atrophy rate estimation. Subsequently, we identified and removed potential outliers by calculating the standardized Z-score for hippocampal volume and excluding observations where the absolute Z-score exceeded 4, a step intended to reduce potential interference from factors such as image segmentation errors. Following this filtering process, hippocampal volumes were re-standardized based on the final analytical sample for use in subsequent statistical models.

Additionally, to ensure the independence of the discovery and validation cohorts, we performed a systematic cross-verification between the ADNI and NACC ADC datasets. We confirmed that there were no overlapping subjects between the two datasets utilized in this study based on unique identi-

fiers and demographic profiles.

#### 2.4 Neuroimaging and Biomarker Definitions

This study utilized pre-computed hippocampal volume data provided by the NACC and ADNI databases. According to the protocols of these repositories, volumetric measures were derived from high-resolution T1-weighted MRI scans using automated segmentation pipelines (primarily FreeSurfer) [17, 50, 51].

For the ADNI longitudinal dataset, images were acquired using both 1.5T and 3T scanners and processed using FreeSurfer versions v4.4, v5.1, or v6.0 depending on the study phase. Specifically for the data utilized in this analysis, hippocampal volumes were adjusted for intracranial volume (ICV) to correct for inter-individual head size differences.

In contrast, the NACC dataset exclusively utilized scans ac-

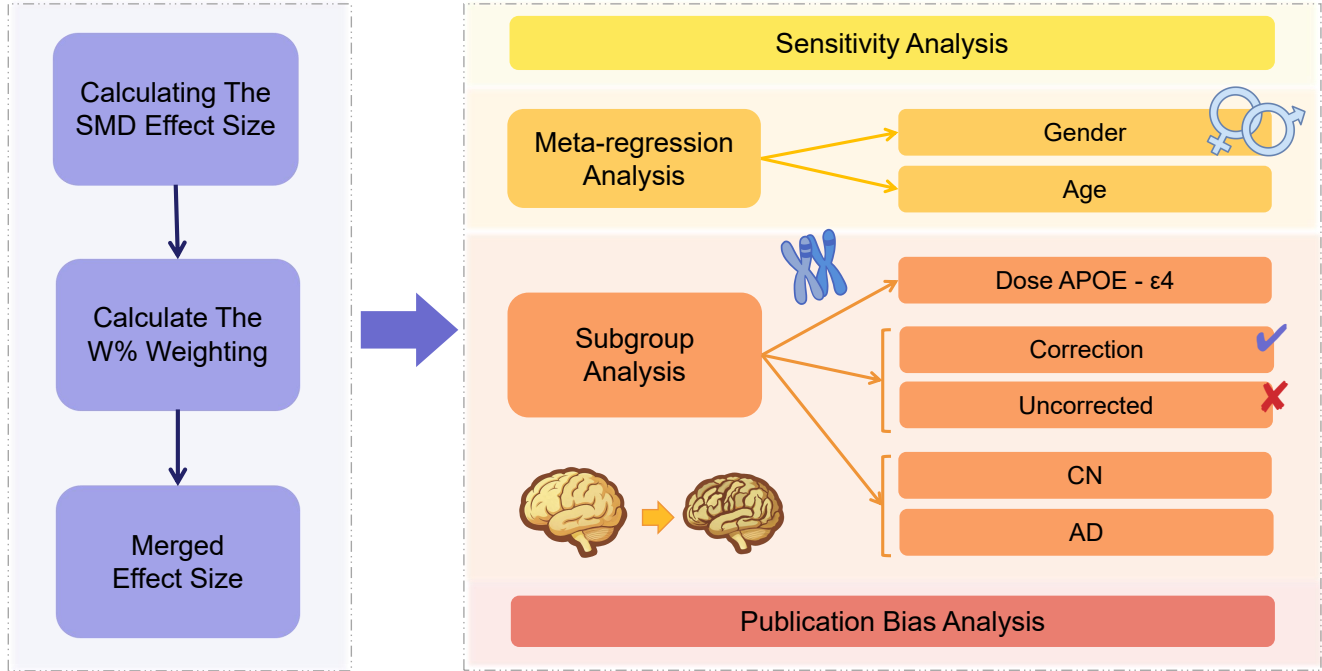


**Figure 2:** Schematic framework of the quantitative synthesis and heterogeneity exploration. The left panel depicts the sequential procedure for pooling effect sizes, moving from individual Standardized Mean Difference (SMD) calculation to weight assignment (W%) and the final merged estimation. The right panel details the strategies employed to investigate heterogeneity, including sensitivity analysis and meta-regression (assessing Gender and Age). Subgroup analyses are stratified by three key domains: APOE- $\epsilon$ 4 genotype dosage, methodological correction (Corrected vs. Uncorrected), and clinical stage (Cognitively Normal, CN; AD). Publication bias assessment is performed as the final validation step.

quired at 3T, processed with the more recent FreeSurfer v7.2. NACC volumes were adjusted using the estimated total intracranial volume (eTIV).

For the ADNI cohort, biomarker positivity was classified using the specific cut-off values provided in the dataset: A $\beta$ 42 < 976.6 pg/mL (Amyloid+), p-Tau181 > 21.8 pg/mL (p-Tau+), and t-Tau > 245 pg/mL (t-Tau+).

## 2.5 Statistical Models

Longitudinal changes in hippocampal volume were analyzed using Linear Mixed-effects Models (LMMs) [52,53]. To account for within-subject correlations and individual heterogeneity in baseline volume and atrophy rates, all models included random intercepts and random slopes for time at the subject level.

*Model 1: Gene-Dose Effect and its Modulators (NACC).* To quantify the dose-dependent acceleration of atrophy associated with APOE- $\epsilon$ 4 and to explore potential modulation by age or sex, we modeled the hippocampal volume trajectories

as follows:

$$\text{Vol}_{ij} = \beta_0 + \beta_1 \text{Time}_{ij} + \beta_2 \text{APOE4}_i \\ + \beta_3 (\text{Time}_{ij} \times \text{APOE4}_i) \\ + \beta_4 (\text{Time}_{ij} \times \text{Age}_i) + \beta_5 (\text{Time}_{ij} \times \text{Sex}_i) \\ + \mathbf{Z}_{ij}\gamma + (u_{0i} + u_{1i} \text{Time}_{ij} + \varepsilon_{ij}) \quad (1)$$

Here,  $\text{Vol}_{ij}$  represents the hippocampal volume for subject  $i$  at time  $j$ . The coefficient  $\beta_3$  captures the additional annual atrophy rate specific to  $\epsilon$ 4 carriers relative to non-carriers. The added interaction terms,  $\beta_4$  and  $\beta_5$ , test whether atrophy rates vary with age or differ by sex, respectively. The term  $\mathbf{Z}_{ij}\gamma$  denotes the main effects of covariates, including Age, Sex, Intracranial Volume (ICV), and Clinical Diagnosis.

*Model 2: Specificity of Synergistic Interaction (ADNI, Individual Models).* To separately test for a synergistic interaction between APOE- $\epsilon$ 4 and each core pathology in the ADNI cohort, we constructed a series of hierarchical models. The

general form for a given biomarker ( $\text{Bio}_k$ ) is:

$$\begin{aligned} \text{Vol}_{ij} = & \beta_0 + \beta_1 \text{Time}_{ij} + \beta_2 \text{APOE4}_i + \beta_3 \text{Bio}_{ki} \\ & + \beta_4 (\text{Time}_{ij} \times \text{APOE4}_i) \\ & + \beta_5 (\text{Time}_{ij} \times \text{Bio}_{ki}) \\ & + \beta_6 (\text{APOE4}_i \times \text{Bio}_{ki}) \\ & + \beta_7 (\text{Time}_{ij} \times \text{APOE4}_i \times \text{Bio}_{ki}) \\ & + \mathbf{Z}_i \boldsymbol{\gamma} + (u_{0i} + u_{1i} \text{Time}_{ij} + \varepsilon_{ij}) \end{aligned} \quad (2)$$

Here,  $\text{APOE4}_i$  is a binary indicator for carrier status, and the three-way interaction coefficient  $\beta_7$  is the primary term of interest.  $\mathbf{Z}$  represent all main effects, two-way interactions, and covariates.

*Model 3: Hierarchy of Synergistic Interaction (ADNI, Joint Model).* To assess the relative influence of  $A\beta$  and p-Tau pathologies, we constructed a joint model that simultaneously included all lower-order terms and the three-way interactions for both pathways:

$$\begin{aligned} \text{Vol}_{ij} = & \beta_0 + \beta_1 \text{Time}_{ij} + \beta_2 \text{APOE4}_i \\ & + \beta_3 A\beta_i + \beta_4 p\text{Tau}_i \\ & + \beta_5 (\text{Time}_{ij} \times \text{APOE4}_i) \\ & + \beta_6 (\text{Time}_{ij} \times A\beta_i) + \beta_7 (\text{Time}_{ij} \times p\text{Tau}_i) \\ & + \beta_8 (\text{APOE4}_i \times A\beta_i) \\ & + \beta_9 (\text{APOE4}_i \times p\text{Tau}_i) \\ & + \beta_A (\text{Time}_{ij} \times \text{APOE4}_i \times A\beta_i) \\ & + \beta_T (\text{Time}_{ij} \times \text{APOE4}_i \times p\text{Tau}_i) \\ & + \mathbf{Z}_i \boldsymbol{\gamma} + (u_{0i} + u_{1i} \text{Time}_{ij} + \varepsilon_{ij}) \end{aligned} \quad (3)$$

This model allows for a direct comparison of the interaction coefficients  $\beta_A$  and  $\beta_T$  after mutual adjustment.

*Mediation Analysis (ADNI).* Given that initial model results suggested the effect of  $\text{APOE-}\epsilon 4$  might be primarily associated with the  $A\beta$  pathway, a mediation analysis was conducted on the ADNI  $\text{APOE-}\epsilon 4$  carriers. This analysis aimed to clarify the mechanistic relationship between  $A\beta$  and p-Tau. First, individual annual atrophy rates were calculated for each carrier. Subsequently, a mediation model was constructed with  $A\beta$  positivity as the independent variable ( $A$ ), baseline p-Tau level as the mediator ( $M$ ), and atrophy rate as the outcome ( $Y$ ), while controlling for covariates. The significance of the indirect effect was assessed using the Sobel test.

## 3 Results

### 3.1 Meta-analysis: Overall Effect and Sources of Heterogeneity

Our quantitative synthesis included 18 eligible studies, which provided 26 distinct cohorts and a total of 4,311 participants. The random-effects meta-analysis showed a significant overall reduction in hippocampal volume for  $\text{APOE-}\epsilon 4$  carriers compared to non-carriers (Standardized Mean Difference [SMD] = -0.27, 95% CI [-0.43, -0.11],  $p = 0.0017$ ).

The analysis indicated substantial heterogeneity across studies ( $I^2 = 61.9\%$ ,  $p < 0.0001$ ), suggesting that the pooled estimate reflects an average effect influenced by underlying moderators and warranting detailed subgroup analyses (Figure 3)(Table 1).

Stratification by clinical diagnosis indicated a pronounced gradient in the magnitude of  $\text{APOE-}\epsilon 4$ -associated atrophy, suggesting that disease stage is a key modulator of the effect size. The association was most pronounced in patients with Alzheimer's Disease, who showed a large and significant volume reduction (SMD = -0.62, 95% CI [-0.94, -0.29],  $p = 0.0037$ ), with reduced heterogeneity in this subgroup ( $I^2 = 34.4\%$ ). In contrast, the effect in Cognitively Normal (CN) individuals was small and not statistically significant (SMD = -0.16, 95% CI [-0.34, 0.02],  $p = 0.071$ ), with considerable remaining heterogeneity ( $I^2 = 55.3\%$ ). This high variability suggests the influence of unmeasured factors, such as the varying prevalence of preclinical amyloid pathology across CN cohorts. We hypothesized that older age, as a proxy for higher amyloid risk, might moderate this effect. However, a specific meta-regression within the CN subgroup did not find a significant association between mean cohort age and effect size ( $p = 0.221$ ). This finding presents a conundrum at the aggregate level: while preclinical pathology is a plausible driver of heterogeneity, this macro-level analysis could not substantiate its link to age. This highlights the limitations of cohort-level data and motivates our subsequent biomarker-stratified longitudinal analysis to resolve this question mechanistically. Following our data processing protocol, only one cohort focused on Mild Cognitive Impairment (MCI) remained, which precluded a pooled subgroup estimate for this intermediate stage.

Further stratification revealed a clear gene-dose effect. Homozygous ( $\epsilon 4/\epsilon 4$ ) carriers exhibited a large and significant reduction in hippocampal volume (SMD = -0.60, 95% CI [-1.08, -0.12],  $p = 0.015$ ), whereas the effect in heterozygous ( $\epsilon 3/\epsilon 4$ ) carriers was negligible and non-significant (SMD = -0.06, 95% CI [-0.31, 0.19],  $p = 0.652$ ). Methodological factors also appeared to influence the results; studies that employed intracranial volume (ICV) correction reported a strong and significant effect (SMD = -0.41, 95% CI [-0.67, -0.16]), whereas uncorrected studies showed a null effect (SMD = -0.10, 95% CI [-0.25, 0.06]).

To investigate sources of heterogeneity across the entire dataset, we performed univariable meta-regressions. We found that neither the mean age of participants ( $p = 0.71$ ) nor the proportion of female participants ( $p = 0.57$ ) were significant moderators of the overall effect size. Sensitivity analyses confirmed the stability of our findings; a multiverse robustness check, which involved sequentially removing the most extreme studies, showed that the overall conclusion remained unchanged. However, a trim-and-fill analysis suggested that smaller, non-significant studies might be underrepresented. The bias-corrected effect size was attenuated and no longer statistically significant (SMD = -0.10, 95% CI [-0.30, 0.10]), warranting caution in interpreting the precise magnitude of



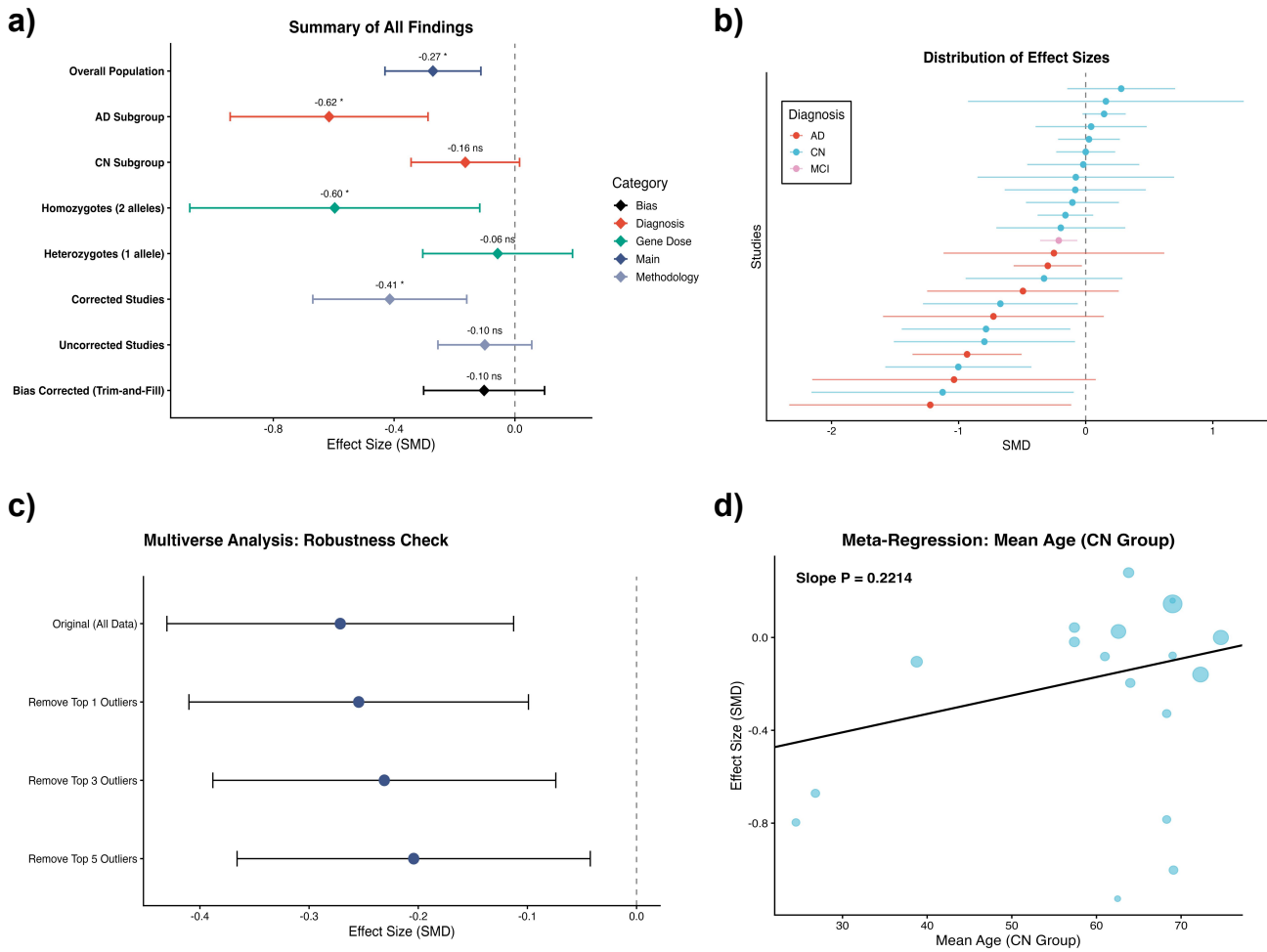


**Figure 3:** Meta-analysis of the association between APOE- $\varepsilon$ 4 and hippocampal volume. (a) Summary forest plot showing the overall pooled Standardized Mean Difference (SMD) and results from key subgroup analyses based on clinical diagnosis (AD, CN), genotype dosage, and methodological correction. A bias-corrected estimate using the trim-and-fill method is also presented. (b) Forest plot illustrating the distribution of effect sizes from all individual studies included in the analysis, color-coded by diagnosis. (c) Multiverse analysis as a robustness check, demonstrating that the overall conclusion remains stable after the sequential removal of the most extreme studies. (d) Meta-regression plot for the Cognitively Normal (CN) subgroup, assessing the moderating effect of mean participant age on the SMD. The non-significant slope ( $p=0.2214$ ) suggests that age does not significantly explain the heterogeneity in this subgroup. In all forest plots, points/diamonds represent SMDs and horizontal lines denote 95% Confidence Intervals (CIs).

## 4 Discussion

This study integrates multi-cohort evidence to address conflicting reports regarding the impact of APOE- $\varepsilon$ 4 on hippocampal integrity. Our findings support a perspective where APOE- $\varepsilon$ 4 functions not as a static risk factor exerting a constant deleterious effect, but as a conditional modulator dependent on the presence of amyloid- $\beta$ .

The heterogeneity identified in our meta-analysis highlights the complexity of detecting this effect in aggregate data. Notably, while we hypothesized that older age, serving as a proxy for increased occult amyloid prevalence, would correlate with larger effect sizes in Cognitively Normal cohorts, our meta-regression did not support this association

( $p = 0.221$ ). This discrepancy between macro-level aggregate data and the expected biological trend likely stems from the ecological fallacy, where mean cohort characteristics obscure individual-level heterogeneity. Consequently, the inability of simple demographic factors to predict atrophy risk in the meta-analysis underscores the critical necessity of our subsequent longitudinal validation. By transitioning from cohort-level aggregates to individual-level biomarker stratification, we resolved this apparent contradiction. We demonstrated that in the absence of A $\beta$ , even older APOE- $\varepsilon$ 4 carriers exhibit atrophy trajectories statistically indistinguishable from non-carriers. This confirms that variable findings in prior literature likely reflect differing prevalences of occult amyloidosis that cannot be captured by age demograph-

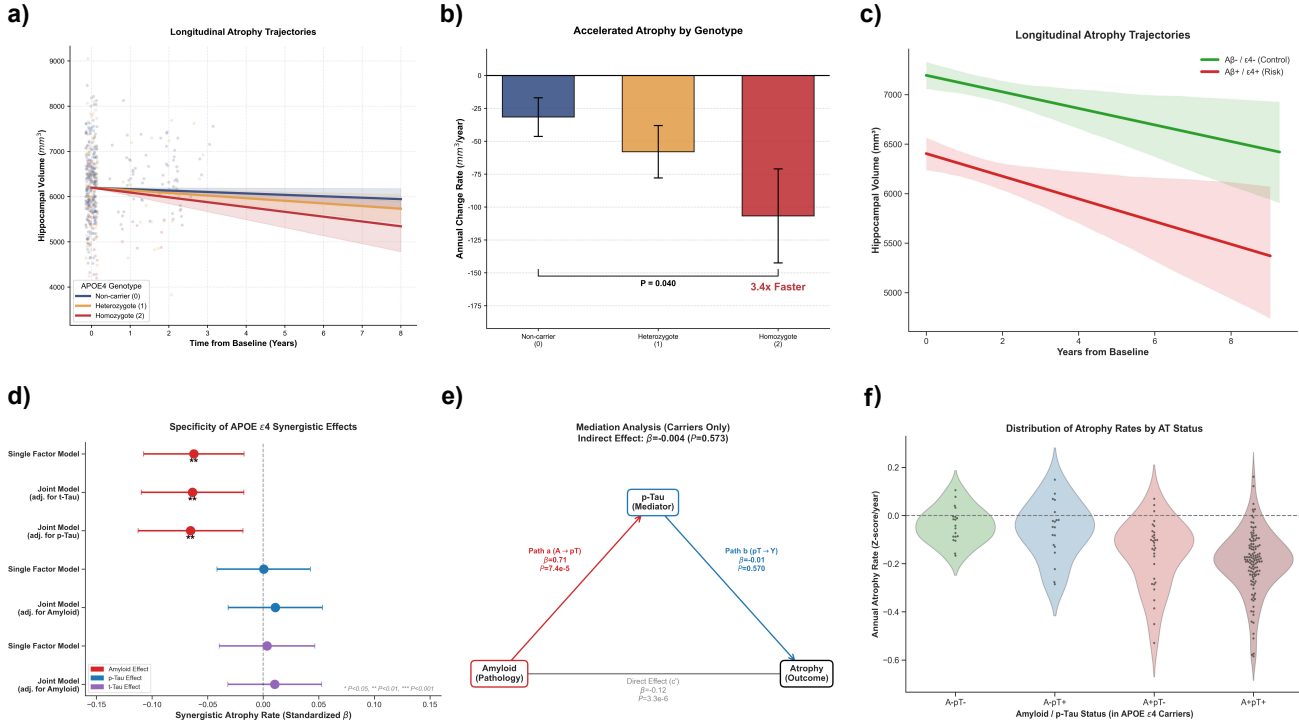


**Figure 4:** Longitudinal hippocampal atrophy trajectories and synergistic interaction effects in the NACC and ADNI cohorts. (a) Estimated longitudinal trajectories of hippocampal volume ( $\text{mm}^3$ ) in the NACC cohort, stratified by APOE- $\epsilon 4$  gene dosage (Non-carrier, Heterozygote, Homozygote). Shaded areas represent 95% Confidence Intervals (CIs). (b) Annualized atrophy rates ( $\text{mm}^3/\text{year}$ ) derived from the NACC Linear Mixed-Effects Model. Bars represent the additional atrophy rate associated with each genotype relative to the non-carrier reference group, quantified by the Time  $\times$  Genotype interaction term. The model indicates a significantly accelerated decline in homozygotes ( $p=0.040$ ). Error bars denote Standard Errors (SE). (c) Estimated longitudinal trajectories in the ADNI cohort, stratified by both Amyloid- $\beta$  ( $A\beta$ ) status and APOE- $\epsilon 4$  carrier status ( $A\beta+/+ \epsilon 4+$  vs. the  $A\beta-/- \epsilon 4-$  control group), illustrating the potent gene-pathology interaction. (d) Forest plot quantifying the specificity of the synergistic interaction effect (Time  $\times$  APOE- $\epsilon 4$   $\times$  Biomarker) on atrophy rates from the ADNI LMMs. The amyloid interaction (red) is significant and remains robust in joint models adjusted for p-Tau or t-Tau, while p-Tau (blue) and t-Tau (purple) interactions are non-significant. Points represent standardized  $\beta$ -coefficients; horizontal lines are 95% CIs. (e) Path diagram of the mediation analysis in APOE- $\epsilon 4$  carriers, testing if the effect of  $A\beta$  pathology on atrophy is mediated by p-Tau. The analysis reveals a non-significant indirect effect ( $p=0.573$ ), supporting a direct association between  $A\beta$  and atrophy. (f) Violin plots showing the distribution of annualized atrophy rates (Z-score/year) among APOE- $\epsilon 4$  carriers stratified by their AT status. Individuals positive for both amyloid and p-Tau ( $A+pT+$ ) exhibit the fastest rates of neurodegeneration.

**Table 2:** Statistical Model Results for Biomarkers

Model	Marker	Coefficient	SE	P-value	$P_{FDR}$
Single Factor Model	$A\beta$	-0.062	0.023	0.007	0.016
Single Factor Model	$p-\tau$	0.000	0.021	0.983	0.983
Single Factor Model	$t-\tau$	0.003	0.022	0.874	0.983
Joint Model (adj. for $p-\tau$ )	$A\beta$	-0.065	0.024	0.007	0.016
Joint Model (adj. for Amyloid)	$p-\tau$	0.011	0.022	0.615	0.882
Joint Model (adj. for $t-\tau$ )	$A\beta$	-0.064	0.024	0.007	0.016
Joint Model (adj. for Amyloid)	$t-\tau$	0.010	0.022	0.630	0.882

Note: SE = Standard Error;  $P_{FDR}$  = False Discovery Rate corrected P-value;  $A\beta$  = Amyloid- $\beta$ ;  $p-\tau$  = phosphorylated tau;  $t-\tau$  = total tau. "adj. for" indicates the model adjusted for the specified covariate.

ics alone. This observation serves as a cautionary note for future meta-analytic studies, warning against reliance on aggregate demographic data and emphasizing the critical need for biomarker-level stratification to achieve mechanistic clarity.

Our analysis of the NACC cohort reveals a crucial non-linearity in the allele dosage effect. We observed a step-wise increase in hippocampal loss characterized by a distinct threshold: homozygous ( $\epsilon 4/\epsilon 4$ ) carriers exhibited a marked acceleration in atrophy, approximately three-fold that of non-carriers, whereas the effect in heterozygotes was minimal and not statistically significant. This suggests that the association of APOE with neurodegeneration is cumulative and threshold-dependent, indicating that homozygosity represents a distinct state of elevated biological risk [54,55].

Mechanistically, our ADNI results provide insight into the drivers of this acceleration. We identified a robust synergistic interaction between APOE- $\epsilon 4$  and A $\beta$  positivity. The mediation analysis indicated that while A $\beta$  strongly predicts p-Tau levels, the accelerated atrophy in carriers was associated directly with A $\beta$ , with no statistically significant indirect effect via soluble p-Tau (p-Tau181). However, this finding warrants cautious interpretation, particularly as our analysis was based on a soluble fluid biomarker. It does not necessarily imply that Tau pathology is biologically irrelevant or absent [56]. Rather, it suggests that in the specific context of APOE- $\epsilon 4$ , the neurodegenerative cascade may not rely exclusively on the sequential amyloid-tau-neurodegeneration pathway captured by fluid biomarkers. Future studies using Tau-PET imaging will be essential to definitively clarify this mediation pathway, as fluid biomarkers may lag behind or behave differently from the aggregated neurofibrillary tangles more proximal to neurodegeneration. A plausible explanation for this direct link involves the innate immune response. Emerging evidence suggests that APOE- $\epsilon 4$  may impair the ability of microglia to contain amyloid plaques, shifting them towards a neurodegenerative phenotype that promotes tissue loss through neuroinflammatory mechanisms [9,57]. These pathways might operate in parallel with, or precede, extensive neurofibrillary tangle formation. Thus, APOE- $\epsilon 4$  may amplify the susceptibility of the brain to amyloid toxicity through pleiotropic mechanisms, creating a scenario where amyloid presence serves as a sufficient trigger for accelerated structural loss [13].

The amyloid-dependent and dose-sensitive relationship described here has implications for disease-modifying therapies. If the structural risk associated with APOE- $\epsilon 4$  is conditional on amyloid burden, therapeutic plaque clearance could theoretically attenuate the acceleration of atrophy [58,59]. Our results suggest this clinical benefit might be most critical for homozygous carriers, who face the steepest natural trajectory of decline, although potential confounders such as amyloid-related imaging abnormalities (ARIA) must be considered [60].

Several limitations should be considered. First, the inability of the meta-regression to detect age effects highlights the noise inherent in aggregating diverse methodological proto-

cols. Second, while we utilized p-Tau181 as a marker, it primarily reflects soluble phosphorylated tau and may not fully capture the burden of insoluble neurofibrillary tangles, potentially underestimating the role of Tau in our mediation model. Future confirmation with Tau-PET imaging will therefore be crucial to investigate the role of aggregated tau pathology in this pathway. Third, the longitudinal cohorts are subject to selection bias, likely representing a healthier subset of the elderly population compared to the general community. Finally, consistent post-processing protocols were prioritized to mitigate measurement variations across scanner versions [61].

## 5 Conclusion

This study characterizes APOE- $\epsilon 4$  as a conditional, dose-dependent accelerator of hippocampal atrophy associated with amyloid pathology. We demonstrate that the limitation of macro-level demographics to predict atrophy risk is resolved by granular, individual-level biomarker profiling. The observed acceleration in homozygous carriers appears driven by a synergistic interaction with amyloid. While our statistical models point to a direct association between A $\beta$  and atrophy in carriers, this likely reflects complex, pleiotropic mechanisms, potentially involving neuroinflammation, where APOE- $\epsilon 4$  exacerbates the neurotoxic response to amyloid. Consequently, clinical risk stratification should integrate amyloid status with allele dosage, and homozygous carriers may represent a priority population for early anti-amyloid interventions to mitigate irreversible structural loss.

## References

- [1] Guy M McKhann, David S Knopman, Howard Chertkow, Bradley T Hyman, Clifford R Jack Jr, Claudia H Kawas, William E Klunk, Walter J Koroshetz, Jennifer J Manly, Richard Mayeux, et al. The diagnosis of dementia due to alzheimer's disease: recommendations from the national institute on aging-alzheimer's association workgroups on diagnostic guidelines for alzheimer's disease. *Alzheimer's & dementia*, 7(3):263–269, 2011.
- [2] Clifford R Jack Jr, David A Bennett, Kaj Blennow, Maria C Carrillo, Billy Dunn, Samantha Budd Haeberlein, David M Holtzman, William Jagust, Frank Jessen, Jason Karlawish, et al. Nia-aa research framework: toward a biological definition of alzheimer's disease. *Alzheimer's & dementia*, 14(4):535–562, 2018.
- [3] Heiko Braak and Eva Braak. Neuropathological staging of alzheimer-related changes. *Acta neuropathologica*, 82(4):239–259, 1991.
- [4] Elizabeth H Corder, Ann M Saunders, Waren J Strittmatter, Donald E Schmeichel, P Craig Gaskell, GWet Small, AD Roses, JL Haines, and Margaret A Pericak-Vance. Gene dose of apolipoprotein e type 4

- allele and the risk of alzheimer's disease in late onset families. *Science*, 261(5123):921–923, 1993.
- [5] Lindsay A Farrer, L Adrienne Cupples, Jonathan L Haines, Bradley Hyman, Walter A Kukull, Richard Mayeux, Richard H Myers, Margaret A Pericak-Vance, Neil Risch, and Cornelia M Van Duijn. Effects of age, sex, and ethnicity on the association between apolipoprotein e genotype and alzheimer disease: a meta-analysis. *Jama*, 278(16):1349–1356, 1997.
- [6] Laurence O'Dwyer, Franck Lamberton, Silke Matura, Colby Tanner, Monika Scheibe, Julia Miller, Dan Rujescu, David Prvulovic, and Harald Hampel. Reduced hippocampal volume in healthy young apoe4 carriers: an mri study. *PloS one*, 7(11):e48895, 2012.
- [7] Rebecca C Knickmeyer, JiaPing Wang, Hongtu Zhu, Xiujuan Geng, Sandra Woolson, Robert M Hamer, Thomas Konneker, Weili Lin, Martin Styner, and John H Gilmore. Common variants in psychiatric risk genes predict brain structure at birth. *Cerebral Cortex*, 24(5):1230–1246, 2014.
- [8] Clifford R Jack, David S Knopman, William J Jagust, Leslie M Shaw, Paul S Aisen, Michael W Weiner, Ronald C Petersen, and John Q Trojanowski. Hypothetical model of dynamic biomarkers of the alzheimer's pathological cascade. *The Lancet Neurology*, 9(1):119–128, 2010.
- [9] Elizabeth C Mormino, Rebecca A Betensky, Trey Hedden, Aaron P Schultz, Rebecca E Amariglio, Dorene M Rentz, Keith A Johnson, and Reisa A Sperling. Synergistic effect of  $\beta$ -amyloid and neurodegeneration on cognitive decline in clinically normal individuals. *JAMA neurology*, 71(11):1379–1385, 2014.
- [10] Naftali Raz, Paolo Ghisletta, Karen M Rodrigue, Kristen M Kennedy, and Ulman Lindenberger. Trajectories of brain aging in middle-aged and older adults: regional and individual differences. *Neuroimage*, 51(2):501–511, 2010.
- [11] Chia-Chen Liu, Takahisa Kanekiyo, Huaxi Xu, and Guojun Bu. Apolipoprotein e and alzheimer disease: risk, mechanisms and therapy. *Nature Reviews Neurology*, 9(2):106–118, 2013.
- [12] Eric M Reiman, Yakeel T Quiroz, Adam S Fleisher, Kewei Chen, Carlos Velez-Pardo, Marlene Jimenez-Del-Rio, Anne M Fagan, Aarti R Shah, Sergio Alvarez, Andrés Arbelaez, et al. Brain imaging and fluid biomarker analysis in young adults at genetic risk for autosomal dominant alzheimer's disease in the presenilin 1 e280a kindred: a case-control study. *The Lancet Neurology*, 11(12):1048–1056, 2012.
- [13] Axel Montagne, Daniel A Nation, Abhay P Sagare, Giuseppe Barisano, Melanie D Sweeney, Ararat Chakhoyan, Maricarmen Pachicano, Elizabeth Joe, Amy R Nelson, Lina M D'Orazio, et al. Apoe4 leads to blood-brain barrier dysfunction predicting cognitive decline. *Nature*, 581(7806):71–76, 2020.
- [14] Reisa A Sperling, Paul S Aisen, Laurel A Beckett, David A Bennett, Suzanne Craft, Anne M Fagan, Takeshi Iwatsubo, Clifford R Jack Jr, Jeffrey Kaye, Thomas J Montine, et al. Toward defining the preclinical stages of alzheimer's disease: Recommendations from the national institute on aging-alzheimer's association workgroups on diagnostic guidelines for alzheimer's disease. *Alzheimer's & dementia*, 7(3):280–292, 2011.
- [15] Prashanthi Vemuri, Heather J Wiste, Stephen D Weigand, David S Knopman, Leslie M Shaw, John Q Trojanowski, Paul S Aisen, Michael Weiner, Ronald C Petersen, Clifford R Jack Jr, et al. Effect of apolipoprotein e on biomarkers of amyloid load and neuronal pathology in alzheimer disease. *Annals of neurology*, 67(3):308–316, 2010.
- [16] Derrek P Hibar, Jason L Stein, Miguel E Renteria, Alejandro Arias-Vasquez, Sylvane Desrivières, Neda Jahanshad, Roberto Toro, Katharina Wittfeld, Lucija Abramovic, Micael Andersson, et al. Common genetic variants influence human subcortical brain structures. *Nature*, 520(7546):224–229, 2015.
- [17] Clifford R Jack Jr, Matt A Bernstein, Nick C Fox, Paul Thompson, Gene Alexander, Danielle Harvey, Bret Borowski, Paula J Britson, Jennifer L Whitwell, Chadwick Ward, et al. The alzheimer's disease neuroimaging initiative (adni): Mri methods. *Journal of Magnetic Resonance Imaging: An Official Journal of the International Society for Magnetic Resonance in Medicine*, 27(4):685–691, 2008.
- [18] Duane L Beekly, Erin M Ramos, William W Lee, Woodrow D Deitrich, Mary E Jacka, Joylee Wu, Janene L Hubbard, Thomas D Koepsell, John C Morris, Walter A Kukull, et al. The national alzheimer's co-ordinating center (nacc) database: the uniform data set. *Alzheimer Disease & Associated Disorders*, 21(3):249–258, 2007.
- [19] Matthew J Page, Joanne E McKenzie, Patrick M Bossuyt, Isabelle Boutron, Tammy C Hoffmann, Cynthia D Mulrow, Larissa Shamseer, Jennifer M Tetzlaff, Elie A Akl, Sue E Brennan, et al. The prisma 2020 statement: an updated guideline for reporting systematic reviews. *bmj*, 372, 2021.
- [20] Wasim Khan, Vincent Giampietro, Tobias Banaschewski, Gareth J Barker, Arun LW Bokde, Christian Buechel, Patricia Conrod, Herta Flor, Vincent Frouin, Hugh Garavan, et al. A multi-cohort study of apoe  $\epsilon$  4 and amyloid- $\beta$  effects on the hippocampus in alzheimer's disease. *Journal of Alzheimer's Disease*, 56(3):1159–1174, 2017.

- [21] Michela Pievani, Samantha Galluzzi, Paul M Thompson, Paul E Rasser, Matteo Bonetti, and Giovanni B Frisoni. Apoe4 is associated with greater atrophy of the hippocampal formation in alzheimer's disease. *Neuroimage*, 55(3):909–919, 2011.
- [22] C Geroldi, M Pihlajamaki, MP Laakso, C DeCarli, A Beltramello, A Bianchetti, H Soininen, M Trabucchi, and Giovanni B Frisoni. Apoe- $\epsilon$ 4 is associated with less frontal and more medial temporal lobe atrophy in ad. *Neurology*, 53(8):1825–1825, 1999.
- [23] Brenda L Plassman, KA Welsh-Bohmer, ED Bigler, SC Johnson, CV Anderson, MJ Helms, AM Saunders, and JCS Breitner. Apolipoprotein e  $\epsilon$ 4 allele and hippocampal volume in twins with normal cognition. *Neurology*, 48(4):985–988, 1997.
- [24] Maheen M Adamson, Kelly M Landy, Susan Duong, Sabrina Fox-Bosetti, J Wesson Ashford, Greer M Murphy, Michael Weiner, and Joy L Taylor. Apolipoprotein e  $\epsilon$ 4 influences on episodic recall and brain structures in aging pilots. *Neurobiology of aging*, 31(6):1059–1063, 2010.
- [25] Mikko Koivumäki, Laura Ekblad, Juan Lantero-Rodriguez, Nicholas J Ashton, Thomas K Karikari, Semi Helin, Riitta Parkkola, Jyrki Löötjönen, Henrik Zetterberg, Kaj Blennow, et al. Blood biomarkers of neurodegeneration associate differently with amyloid deposition, medial temporal atrophy, and cerebrovascular changes in apoe  $\epsilon$ 4-enriched cognitively unimpaired elderly. *Alzheimer's research & therapy*, 16(1):112, 2024.
- [26] H Soininen, K Partanen, A Pitkanen, M Hallikainen, T Hanninen, S Helisalmi, A Mannermaa, M Ryynanen, K Koivisto, and P Riekkinen Sr, MD. Decreased hippocampal volume asymmetry on mris in nondemented elderly subjects carrying the apolipoprotein e  $\epsilon$ 4 allele. *Neurology*, 45(2):391–392, 1995.
- [27] Christopher A Hostage, Kingshuk Roy Choudhury, Pudugramam Murali Doraiswamy, Jeffrey R Petrella, and Alzheimer's Disease Neuroimaging Initiative. Dissecting the gene dose-effects of the apoe  $\epsilon$ 4 and  $\epsilon$ 2 alleles on hippocampal volumes in aging and alzheimer's disease. *PloS one*, 8(2):e54483, 2013.
- [28] Aurélie Bussy, B Joy Snider, Dean Coble, Chengjie Xiong, Anne M Fagan, Carlos Cruchaga, Tammie LS Benzinger, Brian A Gordon, Jason Hassenstab, Randall J Bateman, et al. Effect of apolipoprotein e4 on clinical, neuroimaging, and biomarker measures in noncarrier participants in the dominantly inherited alzheimer network. *Neurobiology of aging*, 75:42–50, 2019.
- [29] Ya-Ting Chang, Hiroaki Kazui, Manabu Ikeda, Chi-Wei Huang, Shu-Hua Huang, Shih-Wei Hsu, Wen-Neng Chang, and Chiung-Chih Chang. Genetic interaction of apoe and fgf1 is associated with memory impairment and hippocampal atrophy in alzheimer's disease. *Aging and disease*, 10(3):510, 2019.
- [30] Panagiotis Alexopoulos, Tanja Richter-Schmidinger, Marco Horn, Sebastian Maus, Martin Reichel, Christos Sidiropoulos, Cosima Rhein, Piotr Lewczuk, Arnd Doerfler, and Johannes Kornhuber. Hippocampal volume differences between healthy young apolipoprotein e  $\epsilon$ 2 and  $\epsilon$ 4 carriers. *Journal of Alzheimer's disease*, 26(2):207–210, 2011.
- [31] Eric M Reiman, Anne Uecker, Richard J Caselli, Stephen Lewis, Daniel Bandy, Mony J De Leon, Susan De Santi, Antonio Convit, David Osborne, Amy Weaver, et al. Hippocampal volumes in cognitively normal persons at genetic risk for alzheimer's disease. *Annals of Neurology: Official Journal of the American Neurological Association and the Child Neurology Society*, 44(2):288–291, 1998.
- [32] T Den Heijer, M Oudkerk, LJ Launer, CM Van Duijn, A Hofman, and MMB Breteler. Hippocampal, amygdalar, and global brain atrophy in different apolipoprotein e genotypes. *Neurology*, 59(5):746–748, 2002.
- [33] Gloria C Chiang, Philip S Insel, Duygu Tosun, Norbert Schuff, Diana Truran-Sacrey, Sky T Raptentset-sang, Paul M Thompson, Eric M Reiman, Clifford R Jack Jr, Nick C Fox, et al. Impact of apolipoprotein  $\epsilon$ -cerebrospinal fluid beta-amyloid interaction on hippocampal volume loss over 1 year in mild cognitive impairment. *Alzheimer's & Dementia*, 7(5):514–520, 2011.
- [34] Erling T Westlye, Arvid Lundervold, Helge Rootwelt, Astri J Lundervold, and Lars T Westlye. Increased hippocampal default mode synchronization during rest in middle-aged and elderly apoe  $\epsilon$ 4 carriers: relationships with memory performance. *Journal of Neuroscience*, 31(21):7775–7783, 2011.
- [35] Tanja Richter-Schmidinger, Panagiotis Alexopoulos, Marco Horn, Sebastian Maus, Martin Reichel, Cosima Rhein, Piotr Lewczuk, Christos Sidiropoulos, Thomas Kneib, Robert Perneczky, et al. Influence of brain-derived neurotrophic-factor and apolipoprotein e genetic variants on hippocampal volume and memory performance in healthy young adults. *Journal of neural transmission*, 118(2):249–257, 2011.
- [36] Hoyoung An, Sang Joon Son, Sooyun Cho, Eun Young Cho, Booyeon Choi, Seong Yoon Kim, Alzheimer's Disease Neuroimaging Initiative, et al. Large intracranial volume accelerates conversion to dementia in males and apoe4 non-carriers with mild cognitive impairment. *International Psychogeriatrics*, 28(5):769–778, 2016.

- [37] Johanna Lind, Anne Larsson, Jonas Persson, Martin Ingvar, Lars-Göran Nilsson, Lars Bäckman, Rolf Adolfsson, Marc Cruts, Kristel Sleegers, Christine Van Broeckhoven, et al. Reduced hippocampal volume in non-demented carriers of the apolipoprotein e ε4: Relation to chronological age and recognition memory. *Neuroscience Letters*, 396(1):23–27, 2006.
- [38] Xiwu Wang, Wenjun Zhou, Teng Ye, Xiaodong Lin, Jie Zhang, and Alzheimer’s Disease Neuroimaging Initiative. The relationship between hippocampal volumes and delayed recall is modified by apoε e4 in mild cognitive impairment. *Frontiers in aging neuroscience*, 11:36, 2019.
- [39] M Lehtovirta, MP Laakso, H Soininen, S Helisalmi, A Mannermaa, E-L Helkala, K Partanen, M Ryynänen, P Vainio, P Hartikainen, et al. Volumes of hippocampus, amygdala and frontal lobe in alzheimer patients with different apolipoprotein e genotypes. *Neuroscience*, 67(1):65–72, 1995.
- [40] Hervé Lemaître, Fabrice Crivello, Carole Dufouil, Blanche Grassiot, Christophe Tzourio, Annick Alpérovitch, and Bernard Mazoyer. No ε4 gene dose effect on hippocampal atrophy in a large mri database of healthy elderly subjects. *Neuroimage*, 24(4):1205–1213, 2005.
- [41] Nicolas Cherbuin, Kaarin J Anstey, Perminder S Sachdev, Jerome J Maller, Chantal Meslin, Holly A Mack, Wei Wen, and Simon Easteal. Total and regional gray matter volume is not related to apoε\* e4 status in a community sample of middle-aged individuals. *The Journals of Gerontology Series A: Biological Sciences and Medical Sciences*, 63(5):501–504, 2008.
- [42] Qunxi Dong, Wen Zhang, Jianfeng Wu, Bolun Li, Emily H Schron, Travis McMahon, Jie Shi, Boris A Gutman, Kewei Chen, Leslie C Baxter, et al. Applying surface-based hippocampal morphometry to study apoε-e4 allele dose effects in cognitively unimpaired subjects. *NeuroImage: Clinical*, 22:101744, 2019.
- [43] Rebecca DerSimonian and Nan Laird. Meta-analysis in clinical trials. *Controlled clinical trials*, 7(3):177–188, 1986.
- [44] Julian PT Higgins and Simon G Thompson. Quantifying heterogeneity in a meta-analysis. *Statistics in medicine*, 21(11):1539–1558, 2002.
- [45] Julian PT Higgins, Simon G Thompson, Jonathan J Deeks, and Douglas G Altman. Measuring inconsistency in meta-analyses. *bmj*, 327(7414):557–560, 2003.
- [46] Matthias Egger, George Davey Smith, Martin Schneider, and Christoph Minder. Bias in meta-analysis detected by a simple, graphical test. *bmj*, 315(7109):629–634, 1997.
- [47] Lilah Besser, Walter Kukull, David S Knopman, Helena Chui, Douglas Galasko, Sandra Weintraub, Gregory Jicha, Cynthia Carlsson, Jeffrey Burns, Joseph Quinn, et al. Version 3 of the national alzheimer’s co-ordinating center’s uniform data set. *Alzheimer Disease & Associated Disorders*, 32(4):351–358, 2018.
- [48] Susanne G Mueller, Michael W Weiner, Leon J Thal, Ronald C Petersen, Clifford R Jack, William Jagust, John Q Trojanowski, Arthur W Toga, and Laurel Beckett. Ways toward an early diagnosis in alzheimer’s disease: the alzheimer’s disease neuroimaging initiative (adni). *Alzheimer’s & Dementia*, 1(1):55–66, 2005.
- [49] Michael W Weiner, Dallas P Veitch, Paul S Aisen, Laurel A Beckett, Nigel J Cairns, Robert C Green, Danielle Harvey, Clifford R Jack Jr, William Jagust, John C Morris, et al. The alzheimer’s disease neuroimaging initiative 3: Continued innovation for clinical trial improvement. *Alzheimer’s & Dementia*, 13(5):561–571, 2017.
- [50] Bruce Fischl. Freesurfer. *Neuroimage*, 62(2):774–781, 2012.
- [51] Bruce Fischl, David H Salat, Evelina Busa, Marilyn Albert, Megan Dieterich, Christian Haselgrove, Andre Van Der Kouwe, Ron Killiany, David Kennedy, Shuna Klaveness, et al. Whole brain segmentation: automated labeling of neuroanatomical structures in the human brain. *Neuron*, 33(3):341–355, 2002.
- [52] Nan M Laird and James H Ware. Random-effects models for longitudinal data. *Biometrics*, pages 963–974, 1982.
- [53] Avital Cnaan, Nan M Laird, and Peter Slasor. Using the general linear mixed model to analyse unbalanced repeated measures and longitudinal data. *Statistics in medicine*, 16(20):2349–2380, 1997.
- [54] Joseph M Castellano, Jungsu Kim, Floy R Stewart, Hong Jiang, Ronald B DeMattos, Bruce W Patterson, Anne M Fagan, John C Morris, Kwasi G Mawuenyega, Carlos Cruchaga, et al. Human apoε isoforms differentially regulate brain amyloid-β peptide clearance. *Science translational medicine*, 3(89):89ra57–89ra57, 2011.
- [55] Susanne Krasemann, Charlotte Madore, Ron Cialic, Caroline Baufeld, Narghes Calcagno, Rachid El Fatimy, Lien Beckers, Elaine O’loughlin, Yang Xu, Zain Fanek, et al. The trem2-apoε pathway drives the transcriptional phenotype of dysfunctional microglia in neurodegenerative diseases. *Immunity*, 47(3):566–581, 2017.
- [56] Renaud La Joie, Adrienne V Visani, Suzanne L Baker, Jesse A Brown, Viktoriya Bourakova, Jungho Cha, Kiran Chaudhary, Lauren Edwards, Leonardo Iaccarino, Mustafa Janabi, et al. Prospective longitudinal atrophy in alzheimer’s disease correlates with the intensity and

- topography of baseline tau-pet. *Science translational medicine*, 12(524):eaau5732, 2020.
- [57] Clifford R Jack Jr, Heather J Wiste, Timothy G Lesnick, Stephen D Weigand, David S Knopman, Prashanthi Ve-muri, Vernon S Pankratz, Matthew L Senjem, Jeffrey L Gunter, Michelle M Mielke, et al. Brain  $\beta$ -amyloid load approaches a plateau. *Neurology*, 80(10):890–896, 2013.
- [58] Christopher H Van Dyck, Chad J Swanson, Paul Aisen, Randall J Bateman, Christopher Chen, Michelle Gee, Michio Kanekiyo, David Li, Larisa Reyderman, Sharon Cohen, et al. Lecanemab in early alzheimer’s disease. *New England Journal of Medicine*, 388(1):9–21, 2023.
- [59] John R Sims, Jennifer A Zimmer, Cynthia D Evans, Ming Lu, Paul Ardayfio, JonDavid Sparks, Alette M Wessels, Sergey Shcherbinin, Hong Wang, Emel Serap Monkul Nery, et al. Donanemab in early symptomatic alzheimer disease: the trailblazer-alz 2 randomized clinical trial. *Jama*, 330(6):512–527, 2023.
- [60] Reisa Sperling, Stephen Salloway, David J Brooks, Donatella Tampieri, Jerome Barakos, Nick C Fox, Murray Raskind, Marwan Sabbagh, Lawrence S Honig, Anton P Porsteinsson, et al. Amyloid-related imaging abnormalities in patients with alzheimer’s disease treated with bapineuzumab: a retrospective analysis. *The Lancet Neurology*, 11(3):241–249, 2012.
- [61] Emily P Hedges, Mihail Dimitrov, Uzma Zahid, Barbara Brito Vega, Shuqing Si, Hannah Dickson, Philip McGuire, Steven Williams, Gareth J Barker, and Matthew J Kempton. Reliability of structural mri measurements: The effects of scan session, head tilt, inter-scan interval, acquisition sequence, freesurfer version and processing stream. *Neuroimage*, 246:118751, 2022.

## Funding

This work was supported by the Natural Science Foundation of Xinjiang Uygur Autonomous Region (Grant No. 2024D01C216), the “Tianchi Talents” Introduction Plan, and the National University Student Innovation Practice Program.

## Acknowledgments

The authors extend their sincere gratitude to their colleagues and mentors, as well as to Shenzhen X-Institute and Xinjiang University, for their invaluable discussions and support.

Data collection and sharing for the Alzheimer’s Disease Neuroimaging Initiative (ADNI) is funded by the National Institute on Aging (National Institutes of Health Grant U19AG024904). The grantee organization is the Northern California Institute for Research and Education. In the past, ADNI has also received funding from the National Institute of Biomedical Imaging and Bioengineering, the Canadian Institutes of Health Research, and private sector contributions

through the Foundation for the National Institutes of Health (FNIH) including generous contributions from the following: AbbVie, Alzheimer’s Association; Alzheimer’s Drug Discovery Foundation; Araclon Biotech; BioClinica, Inc.; Biogen; Bristol-Myers Squibb Company; CereSpir, Inc.; Cogstate; Eisai Inc.; Elan Pharmaceuticals, Inc.; Eli Lilly and Company; EuroImmun; F. Hoffmann-La Roche Ltd and its affiliated company Genentech, Inc.; Fujirebio; GE Healthcare; IXICO Ltd.; Janssen Alzheimer Immunotherapy Research & Development, LLC.; Johnson & Johnson Pharmaceutical Research & Development LLC.; Lumosity; Lundbeck; Merck & Co., Inc.; Meso Scale Diagnostics, LLC.; NeuroRx Research; Neurotrack Technologies; Novartis Pharmaceuticals Corporation; Pfizer Inc.; Piramal Imaging; Servier; Takeda Pharmaceutical Company; and Transition Therapeutics.

The NACC database is funded by NIA/NIH Grant U24 AG072122. SCAN is a multi-institutional project that was funded as a U24 grant (AG067418) by the National Institute on Aging in May 2020. Data collected by SCAN and shared by NACC are contributed by the NIA-funded ADRCs as follows: Arizona Alzheimer’s Center - P30 AG072980 (PI: Eric Reiman, MD); R01 AG069453 (PI: Eric Reiman (contact), MD); P30 AG019610 (PI: Eric Reiman, MD); and the State of Arizona which provided additional funding supporting our center; Boston University - P30 AG013846 (PI Neil Kowall MD); Cleveland ADRC - P30 AG062428 (James Leverenz, MD); Cleveland Clinic, Las Vegas – P20AG068053; Columbia - P50 AG008702 (PI Scott Small MD); Duke/UNC ADRC – P30 AG072958; Emory University - P30AG066511 (PI Levey Allan, MD, PhD); Indiana University - R01 AG19771 (PI Andrew Saykin, PsyD); P30 AG10133 (PI Andrew Saykin, PsyD); P30 AG072976 (PI Andrew Saykin, PsyD); R01 AG061788 (PI Shannon Risacher, PhD); R01 AG053993 (PI Yu-Chien Wu, MD, PhD); U01 AG057195 (PI Liana Apostolova, MD); U19 AG063911 (PI Bradley Boeve, MD); and the Indiana University Department of Radiology and Imaging Sciences; Johns Hopkins - P30 AG066507 (PI Marilyn Albert, PhD.); Mayo Clinic - P50 AG016574 (PI Ronald Petersen MD PhD); Mount Sinai - P30 AG066514 (PI Mary Sano, PhD); R01 AG054110 (PI Trey Hedden, PhD); R01 AG053509 (PI Trey Hedden, PhD); New York University - P30AG066512-01S2 (PI Thomas Wisniewski, MD); R01AG056031 (PI Ricardo Osorio, MD); R01AG056531 (PIs Ricardo Osorio, MD; Girardin Jean-Louis, PhD); Northwestern University - P30 AG013854 (PI Robert Vassar PhD); R01 AG045571 (PI Emily Rogalski, PhD); R56 AG045571, (PI Emily Rogalski, PhD); R01 AG067781, (PI Emily Rogalski, PhD); U19 AG073153, (PI Emily Rogalski, PhD); R01 DC008552, (M.-Marsel Mesulam, MD); R01 AG077444, (PIs M.-Marsel Mesulam, MD, Emily Rogalski, PhD); R01 NS075075 (PI Emily Rogalski, PhD); R01 AG056258 (PI Emily Rogalski, PhD); Oregon Health & Science University - P30 AG066518 (PI Lisa Silbert, MD, MCR); Rush University - P30 AG010161 (PI David Bennett MD); Stanford – P30AG066515; P50 AG047366 (PI Victor Henderson MD MS); University of Alabama,

Birmingham – P20; University of California, Davis - P30 AG10129 (PI Charles DeCarli, MD); P30 AG072972 (PI Charles DeCarli, MD); University of California, Irvine - P50 AG016573 (PI Frank LaFerla PhD); University of California, San Diego - P30AG062429 (PI James Brewer, MD, PhD); University of California, San Francisco - P30 AG062422 (Rabinovici, Gil D., MD); University of Kansas - P30 AG035982 (Russell Swerdlow, MD); University of Kentucky - P30 AG028283-15S1 (PIs Linda Van Eldik, PhD and Brian Gold, PhD); University of Michigan ADRC - P30AG053760 (PI Henry Paulson, MD, PhD) P30AG072931 (PI Henry Paulson, MD, PhD) Cure Alzheimer's Fund 200775 - (PI Henry Paulson, MD, PhD) U19 NS120384 (PI Charles DeCarli, MD, University of Michigan Site PI Henry Paulson, MD, PhD) R01 AG068338 (MPI Bruno Giordani, PhD, Carol Persad, PhD, Yi Murphey, PhD) S10OD026738-01 (PI Douglas Noll, PhD) R01 AG058724 (PI Benjamin Hampstead, PhD) R35 AG072262 (PI Benjamin Hampstead, PhD) W81XWH2110743 (PI Benjamin Hampstead, PhD) R01 AG073235 (PI Nancy Chiaravalloti, University of Michigan Site PI Benjamin Hampstead, PhD) 1I01RX001534 (PI Benjamin Hampstead, PhD) IRX001381 (PI Benjamin Hampstead, PhD); University of New Mexico - P20 AG068077 (Gary Rosenberg, MD); University of Pennsylvania - State of PA project 2019NF4100087335 (PI David Wolk, MD); Rooney Family Research Fund (PI David Wolk, MD); R01 AG055005 (PI David Wolk, MD); University of Pittsburgh - P50 AG005133 (PI Oscar Lopez MD); University of Southern California - P50 AG005142 (PI Helena Chui MD); University of Washington - P50 AG005136 (PI Thomas Grabowski MD); University of Wisconsin - P50 AG033514 (PI Sanjay Asthana MD FRCP); Vanderbilt University – P20 AG068082; Wake Forest - P30AG072947 (PI Suzanne Craft, PhD); Washington University, St. Louis - P01 AG03991 (PI John Morris MD); P01 AG026276 (PI John Morris MD); P20 MH071616 (PI Dan Marcus); P30 AG066444 (PI John Morris MD); P30 NS098577 (PI Dan Marcus); R01 AG021910 (PI Randy Buckner); R01 AG043434 (PI Catherine Roe); R01 EB009352 (PI Dan Marcus); UL1 TR000448 (PI Brad Evanoff); U24 RR021382 (PI Bruce Rosen); Avid Radiopharmaceuticals / Eli Lilly; Yale - P50 AG047270 (PI Stephen Strittmatter MD PhD); R01AG052560 (MPI: Christopher van Dyck, MD; Richard Carson, PhD); R01AG062276 (PI: Christopher van Dyck, MD); 1Florida - P30AG066506-03 (PI Glenn Smith, PhD); P50 AG047266 (PI Todd Golde MD PhD).

The Alzheimer's Disease Genetics Consortium (ADGC) is funded by a grant from the National Institute on Aging (PI, Gerard D. Schellenberg; UO1AG032984).

## Code Availability

The analysis code for this paper is available at the GitHub repository: <https://github.com/wyqmath/admeta>.

## Conflict of Interest Statement

The authors declare that the research was conducted in the absence of any commercial or financial relationships that could be construed as a potential conflict of interest.

## A Supporting Information

### A.1 Search Strategy and Study Selection

A comprehensive literature search was conducted in four electronic databases from their inception to August 2025: PubMed, Embase (via Ovid), the Cochrane Library, and Web of Science (Science Citation Index Expanded and Emerging Sources Citation Index). The search was limited to publications in English. The search strategy combined subject headings (MeSH in PubMed, Emtree in Embase) with free-text keywords covering two core concepts: (1) Alzheimer's disease and related terms; and (2) Apolipoprotein E  $\epsilon 4$  (APOE  $\epsilon 4$ ) carrier status. No methodological filters for study design were applied during the search phase to maximize sensitivity. The complete search queries for all databases are detailed in Supplementary Table S1.

All retrieved records were first imported into EndNote for reference management and automated deduplication. Subsequently, the screening process was conducted in two stages by two independent researchers. In the first stage, titles and abstracts were screened to exclude reviews, meta-analyses, animal studies, letters, case reports, conference proceedings, and literature clearly irrelevant to the research topic. In the second stage, the remaining records were uploaded to the web-based systematic review platform Covidence (<https://www.covidence.org/>) for full-text assessment. These two researchers independently reviewed the full texts against specific eligibility criteria, which are detailed in the following section. To ensure the independence of data, we rigorously checked publications to identify potential population overlap. When multiple articles reported on the same or highly similar datasets, we included only the one with the largest sample size or the most recent publication date. Any discrepancies during the screening process were resolved through discussion or by a third researcher's adjudication. The entire screening process is reported in a PRISMA 2020 flow diagram.

### A.2 Data Extraction

Two researchers independently extracted data from the included studies using a pre-designed standardized data extraction form. Any disagreements were resolved by consulting a third researcher. We extracted the following demographic and clinical characteristics: sample size, mean age, sex ratio, and APOE  $\epsilon 4$  gene dosage information for each experimental group. The primary outcome measures extracted included total hippocampal volume, as well as left and right hippocampal volumes separately. For studies that only reported left and right hippocampal volumes without the total volume, we used a standard formula incorporating the correlation coefficient to calculate the mean and standard deviation of the total hippocampal volume, correcting for the correlation between the two hemispheres. To address potential methodological heterogeneity, we also recorded detailed information regarding MRI image acquisition and processing. This included: (1) the specific MRI processing software used; (2) the hippocam-

pal segmentation method (manual tracing vs. automated segmentation); (3) whether hippocampal volumes were corrected for intracranial volume (ICV) to account for individual differences in head size, and the specific correction method used; and (4) whether longitudinal data processing was included.

### A.3 Eligibility Criteria

The inclusion and exclusion criteria were established *a priori* based on the PICOS (Population, Intervention/Exposure, Comparator, Outcomes, Study design) framework and reported according to the PRISMA guidelines.

#### A.3.1 Inclusion Criteria

Studies were considered eligible for inclusion if they met the following criteria:

- 1. Study Design:** The study design was cross-sectional or provided baseline data from longitudinal cohorts comparing APOE  $\epsilon 4$  carriers versus non-carriers.
- 2. Population:** Participants were human adults diagnosed with Alzheimer's disease (AD), Mild Cognitive Impairment (MCI), or were Cognitively Normal (CN) based on established clinical criteria (e.g., NINCDS-ADRDA, NIA-AA).
- 3. Outcome:** The study reported quantitative measurements of hippocampal volume derived from Magnetic Resonance Imaging (MRI), regardless of the segmentation method (manual or automated) or intracranial volume (ICV) correction status.
- 4. Data Availability:** Sufficient statistical data were provided, specifically the sample size ( $N$ ), mean hippocampal volume, and standard deviation ( $SD$ ) or standard error ( $SE$ ) for both genotype groups to allow for the calculation of effect sizes.
- 5. Publication Type:** The article was an original research paper published in English.

#### A.3.2 Exclusion Criteria

Studies were excluded based on the following criteria:

- 1. Non-Original Research:** Non-original research, including reviews, meta-analyses, conference abstracts, letters, editorials, or case reports.
- 2. Participants:** Studies involving animal models or *in vitro* experiments, or studies focusing on participants with other neurological or psychiatric disorders (e.g., Parkinson's disease, vascular dementia) that could confound hippocampal atrophy assessments.
- 3. Data Quality:** Publications with insufficient or irretrievable data where the Standardized Mean Difference ( $SMD$ ) could not be calculated.
- 4. Data Overlap:** Studies utilizing overlapping datasets or cohorts. In cases where multiple studies reported on

the same population (e.g., overlapping samples from the ADNI database), priority was given to the study with the largest sample size or the most recent publication date to avoid data duplication.

**Table S1:** Detailed Search Strategies for Electronic Databases (Search Date: August 2025)

Database	Search Strategy
<b>1. PubMed</b>	
#1	"Alzheimer Disease"[Mesh] OR "Alzheimer*"[Title/Abstract] OR "Alzheimer's"[Title/Abstract] OR "AD"[Title/Abstract] OR "Senile Dementia"[Title/Abstract] OR "Presenile Dementia"[Title/Abstract] OR "Alzheimer Type Dementia"[Title/Abstract] OR "FAD"[Title/Abstract] OR "Familial Alzheimer Disease"[Title/Abstract] OR "Early Onset Alzheimer*"[Title/Abstract] OR "Late Onset Alzheimer*"[Title/Abstract]
#2	"Apolipoprotein E4"[Mesh] OR "Apolipoprotein E"[Mesh] OR "APOE"[Title/Abstract] OR "APOE4"[Title/Abstract] OR "ApoE-4"[Title/Abstract] OR "epsilon 4"[Title/Abstract] OR "e4 allele"[Title/Abstract] OR "Apo E"[Title/Abstract]
#3	"Hippocampus"[Mesh] OR "Hippocamp*"[Title/Abstract] OR "Hippocampal Volume"[Title/Abstract] OR "Hippocampal Atrophy"[Title/Abstract]
#4	"Magnetic Resonance Imaging"[Mesh] OR "MRI"[Title/Abstract] OR "Neuroimaging"[Title/Abstract] OR "Voxel-based morphometry"[Title/Abstract] OR "Volumetric"[Title/Abstract] OR "Brain Volume"[Title/Abstract]
#5	#3 AND #4
#6	#1 AND #2 AND #5
<b>2. Embase</b>	
#1	'alzheimer disease'/exp OR 'alzheimer*':ti,ab,kw OR 'senile dementia':ti,ab,kw OR 'presenile dementia':ti,ab,kw OR 'ad':ti,ab,kw OR 'familial alzheimer disease':ti,ab,kw
#2	'apolipoprotein E4'/exp OR 'apoe':ti,ab,kw OR 'apoe4':ti,ab,kw OR 'apolipoprotein e':ti,ab,kw OR 'epsilon 4':ti,ab,kw
#3	'hippocampus'/exp OR 'hippocamp*':ti,ab,kw OR 'hippocampal atrophy':ti,ab,kw OR 'hippocampal volume':ti,ab,kw
#4	'nuclear magnetic resonance imaging'/exp OR 'mri':ti,ab,kw OR 'magnetic resonance imaging':ti,ab,kw
#5	#1 AND #2 AND #3 AND #4
<b>3. Web of Science</b>	
#1	TS=(“Alzheimer*” OR “AD” OR “Senile Dementia” OR “Presenile Dementia” OR “Alzheimer Type Dementia” OR “FAD”)
#2	TS=(“Apolipoprotein E” OR “APOE” OR “APOE4” OR “epsilon 4” OR “Apo E4”)
#3	TS=(“Hippocampus” OR “Hippocampal” OR “Hippocampal Volume” OR “Hippocampal Atrophy”)
#4	TS=(“MRI” OR “Magnetic Resonance Imaging” OR “Brain Volume”)
#5	#1 AND #2 AND #3 AND #4
<b>4. Cochrane Library</b>	
#1	MeSH descriptor: [Alzheimer Disease] explode all trees
#2	(Alzheimer* OR "Senile Dementia" OR "Presenile Dementia" OR "Alzheimer Type Dementia" OR "FAD" OR "Familial Alzheimer Disease"):ti,ab,kw
#3	#1 OR #2
#4	MeSH descriptor: [Apolipoprotein E4] explode all trees
#5	MeSH descriptor: [Apolipoproteins E] explode all trees
#6	(APOE* OR "Apolipoprotein E" OR "Apolipoprotein E4" OR "epsilon 4" OR "e4 allele"):ti,ab,kw
#7	#4 OR #5 OR #6
#8	MeSH descriptor: [Hippocampus] explode all trees
#9	(Hippocamp* OR "Hippocampal Volume" OR "Hippocampal Atrophy"):ti,ab,kw
#10	#8 OR #9
#11	MeSH descriptor: [Magnetic Resonance Imaging] explode all trees
#12	(MRI OR "Magnetic Resonance Imaging" OR "Brain Volume" OR Volumetric OR "Voxel-based morphometry"):ti,ab,kw
#13	#11 OR #12
#14	#3 AND #7 AND #10 AND #13

**Table S2:** Characteristics of Included Studies for Meta-Analysis

Study ID	Sample Size	Age (Mean $\pm$ SD)	Gender (% Male)	Included Diagnosis
[20] Khan et al., 2017	1781	74.4 (Weighted Mean)	49.6	AD, MCI, CN
[21] Pievani et al., 2011	56	71.1 $\pm$ 8.3	32.1	AD, CN
[22] Geroldi et al., 1999	58	70.7 $\pm$ 8.7	27.6	AD, CN
[23] Plassman et al., 1997	20	62.5 $\pm$ 7.8	30	CN
[24] Adamson et al., 2010	50	61.0 $\pm$ 6.7	82	CN
[42] Dong et al., 2019	117	58.1 $\pm$ 6.1	38.5	CN
[25] Koivumäki et al., 2024	59	67.6 $\pm$ 4.7	36.7	CN
[26] Soininen et al., 1995	32	69 $\pm$ 6	31.3	CN
[27] Hostage et al., 2013	662	75.3 $\pm$ 6.6	58.2	AD, MCI, CN
[28] Bussy et al., 2019	162	38.8 $\pm$ 11.7	39.5	CN
[29] Chang et al., 2019	97	71.5 $\pm$ 7.8	54.6	AD
[30] Alexopoulos et al., 2011	33	24.5 $\pm$ 3.6	36.4	CN
[31] Reiman et al., 1998	33	50–62 (Range)	NR	CN
[32] Den Heijer et al., 2002	428	72.3 $\pm$ 7.0	47.8	CN
[33] Chiang et al., 2011	297	74.9 $\pm$ 7.2	59.9	AD, MCI, CN
[34] Westlye et al., 2011	95	63.8 $\pm$ 7.2	35.8	CN
[35] Richter-Schmidinger et al., 2011	135	24.5 $\pm$ 3.2	32.6	CN
[36] An et al., 2016	637	72.3 $\pm$ 7.4	58.4	MCI
[6] O'Dwyer et al., 2012	44	26.8 $\pm$ 4.6	59.1	CN
[37] Lind et al., 2006	60	66.0 $\pm$ 8.1	38.3	CN
[38] Wang et al., 2019	1347	73.6 $\pm$ 7.1	55.8	AD, MCI, CN
[39] Lehtovirta et al., 1995	42	69.4 $\pm$ 7.5	47.6	AD, CN
[40] Lemaître et al., 2005	750	69.4 $\pm$ 2.9	42	CN
[41] Cherbuin et al., 2008	331	62.6 $\pm$ 1.4	53.5	CN

**Table S3:** Full Results of the Linear Mixed-Effects Model on NACC Data

Predictor	Coefficient	Std. Error	z-value	P-value	95% Confidence Interval
<i>Fixed Effects</i>					
Intercept	3693.02	101.95	36.22	< 0.001	[3493.20, 3892.84]
<i>APOE4 Dosage (Ref: Non-carrier)</i>					
Heterozygote (1)	-98.29	25.02	-3.93	< 0.001	[-147.33, -49.25]
Homozygote (2)	-342.35	51.31	-6.67	< 0.001	[-442.91, -241.79]
Sex (Ref: Female) [Male]	227.65	28.14	8.09	< 0.001	[172.50, 282.79]
<i>Baseline Diagnosis (Ref: CN)</i>					
AD	-721.25	44.22	-16.31	< 0.001	[-807.92, -634.57]
MCI	-284.91	28.33	-10.06	< 0.001	[-340.43, -229.39]
Time	-31.61	14.68	-2.15	0.031	[-60.38, -2.84]
Time × APOE4 Heterozygote	-26.37	21.62	-1.22	0.223	[-68.76, 16.01]
Time × APOE4 Homozygote	-75.11	36.49	-2.06	0.040	[-146.63, -3.60]
Time × Sex [Male]	-28.40	19.91	-1.43	0.154	[-67.43, 10.63]
Age (Centered)	-23.98	1.38	-17.33	< 0.001	[-26.69, -21.27]
Time × Age (Centered)	-3.44	1.25	-2.75	0.006	[-5.89, -0.99]
eTIV (Scaled)	1.75	0.07	24.10	< 0.001	[1.61, 1.89]
<i>Random Effects Variance Components</i>					
Group Variance	15.79				
Group × Time Covariance	-0.81				
Time Variance	1.65				

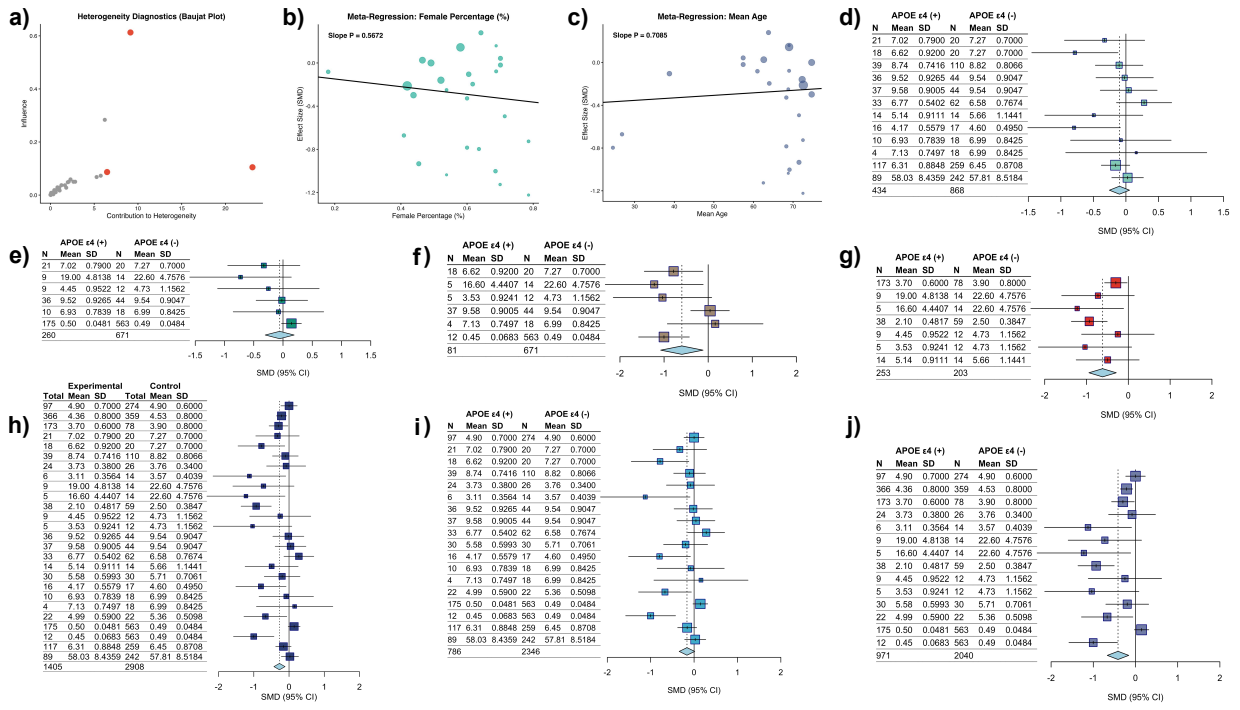


**Figure S1:** Supplementary plots for the meta-analysis. (a) Baujat plot for heterogeneity diagnostics, identifying influential studies. (b-c) Meta-regression plots showing the relationship between effect size (SMD) and moderators: (b) percentage of female participants and (c) mean age. (d-j) Forest plots visualizing the effect size of APOE ε4 on hippocampal volume across different subgroups and methodologies.